

Rayleigh scattering of neutron capture γ rays from lead

Sylvian Kahane

Physics Department, Nuclear Research Center-Negev, P.O. Box 9001, Beer Sheva, Israel

R. Moreh

*Physics Department, Nuclear Research Center-Negev, P.O. Box 9001, Beer Sheva, Israel
and Physics Department, Ben-Gurion University, Beer Sheva, Israel*

O. Shahal

Physics Department, Nuclear Research Center-Negev, P.O. Box 9001, Beer Sheva, Israel

(Received 3 February 1992)

Nineteen γ lines in the energy range 465–2842 keV, produced by the $\text{Ni}(n,\gamma)$ and $\text{Fe}(n,\gamma)$ reactions, were scattered from a natural Pb target at angles of $\theta=1.02^\circ$ for the Ni source and $\theta=1.80^\circ$ for the Fe source. Differential cross sections were measured relative to carbon and are dominated completely by Rayleigh scattering. The results were found to agree well with the modified relativistic form-factor calculations within 5%.

PACS number(s): 32.80.Cy, 29.90.+r

I. INTRODUCTION

The Rayleigh effect is elastic photon scattering by the electron cloud of an atom in the presence of the static potential field generated by the nucleus and the electrons themselves. As the name suggests, this is quite an old scattering effect, at first addressed by Lord Rayleigh [1] in his immortal questions, “Why is the sky blue?” or, alternatively, “Why are the sunsets red?” Using classical electrodynamics, an ω^4 law was obtained for the scattering cross section [2] of the visible light by the atmosphere. This strong dependence on the photon energy answers very well both of the above somewhat poetical concerns of Lord Rayleigh. With the advent of quantum electrodynamics, the name was generalized to the whole photon spectrum and its interaction with the atomic electrons, in contrast to other interactions of a nuclear nature. Rayleigh scattering competes, coherently, with other elastic-scattering processes; namely, Delbrück scattering, which is scattering by the bare Coulomb field of the nucleus; nuclear Thomson scattering, which is elastic scattering by the charge distribution of the nucleus; and nuclear resonance scattering (known also as nuclear Rayleigh scattering), in which nuclear collective degrees of freedom are excited; and via deexcitation back to the ground state elastic scattering occurs. Each of these processes possesses characteristic dependencies on energy, scattering angle, and nuclear charge. In general, analysis of an elastic-scattering experiment is hindered by the complicated interference patterns [3] of the various contributing effects. Rayleigh scattering remains at the center of scientific interest because it can be applied as a quantitative tool in plasma diagnostics.

Recently we published a measurement from U [4], in which the Rayleigh effect was the dominant contribution by orders of magnitude over the other scattering processes,

isolating its contribution. In this way accurate comparison with existing theories was made possible. Briefly, 19 neutron-capture γ rays from 0.46 MeV to 2.84 MeV, produced in the $\text{Ni}(n,\gamma)$ and $\text{Fe}(n,\gamma)$ reactions, were elastically scattered at forward angles in the 1° – 2° range, covering momentum transfers from 0.3 to 2.2 \AA^{-1} .

In the present work we report on a similar measurement from a Pb target, under the same experimental conditions. Lead is probably the most frequently and thoroughly investigated target in what concerns Rayleigh scattering; a summary of the existing experiments is presented in Table I. Being a second-order effect (one photon in, one photon out), Rayleigh scattering has to be calculated in second-order quantum electrodynamics (S -matrix theory). Such a calculation will produce separate dependencies on θ , the scattering angle, and ω , the photon energy. The fascinating approximations of the form-factor and modified-form-factor type combine these two parameters into one: q , the momentum transfer. Therefore it is crucial to study the Rayleigh scattering, in as a wide range as possible, of θ , ω , and q to assess and understand the validity of these approximations. On practical grounds, it is to be noted that the full S -matrix calculations are very difficult to perform, and hence, form-factor approximations are the only practical theoretical means easily available. One can see that our experiment has some momentum-transfer overlap with that of Eichler and de Barros [5], and almost complete overlap with that of Lestone *et al.* [20]. The latter experiment has also other common features with ours: (i) use of multiple γ -line sources the same measurement, (ii) a large span of energies (theirs 1.1 MeV, ours 2.4 MeV), and (iii) forward-angles scattering. Energetically we overlap only with the experiment of Lestone *et al.* (but our range is wider); and, in what concerns the scattering angle, our experiment is unique by the virtue of the very small forward angles achieved (1.02° and 1.80°).

TABLE I. Summary of the existing experimental Rayleigh scattering measurements from lead.

Energy (keV)	q (\AA^{-1})	Angular range	Reference
59.54	0.8–3.8	20°–110°	Eichler and de Barros [5]
59.54	2.4–4.6	60°–150°	Schumacher and Stoffregen [6]
145.4	2.5–5.8	25°–60°	Eichler <i>et al.</i> [7]
145.4	1.5–4.0	15°–40°	de Barros <i>et al.</i> [8]
145.4	4.5–9.9	45°–115°	Prasad <i>et al.</i> [9]
145.4	3.2–11.3	30°–150°	Schumacher [10]
279.2	2.1–11.1	10°–60°	Bradley and Ghose [11]
279.2	6.2–21.7	30°–150°	Smend, Schumacher, and Borchert [12]
411.8	9.1–32.1	30°–150°	Schumacher [10]
468.0	1.7–12.9	5°–40°	de Barros <i>et al.</i> [13]
661.6	4.9–26.3	10°–60°	Bradley and Ghose [11]
661.6	14.7–51.5	30°–150°	Smend, Schumacher, and Borchert [12]
889.3	19.8–69.3	30°–150°	Schumacher, Smend, and Borchert [14]
1332.5	27.8–103.8	30°–150°	Dixon and Storey [15]
1332.5	53.7–99.3	60°–135°	Hardie, Merrow, and Schwardt [16]
1332.5	11.2–53.7	10°–60°	Hardie, De Vries, and Chiang [17]
1332.5	2.8–9.1	3°–10°	Basavaraju <i>et al.</i> [18]
1332.5	4.2–11.3	5°–12°	Kane <i>et al.</i> [19]
Multiline γ source	0.5–43.5	2°–10°	Lestone <i>et al.</i> [20]

II. THEORETICAL REMARKS

A formal expression for the second-order quantum electrodynamics S matrix, specialized to the Rayleigh scattering case, is given by [2]

$$S_{fi} = \frac{ir_0}{2\pi\omega} \sum_I \left[\frac{\langle i | \alpha \epsilon_f^* e^{-ik_f \cdot r} | I \rangle \langle I | \alpha \epsilon_i e^{ik_i \cdot r} | i \rangle}{E_I - E_i - \omega} + \frac{\langle i | \alpha \epsilon_i e^{ik_i \cdot r} | I \rangle \langle I | \alpha \epsilon_f^* e^{-ik_f \cdot r} | i \rangle}{E_I - E_i + \omega} \right], \quad (1)$$

where ϵ is the polarization vector, ω the photon energy, E the electron energy, α the Dirac matrix, and $|i\rangle$ the multielectron initial (and, in this case, final) states.

This expression was used, in various degrees of approximation, to calculate *exact* Rayleigh scattering amplitudes. Brown, Peierles, and Woodward [22] and Cornille and Chapdelaine [23] used pure Coulomb fields; Florescu and Gavrilă [24] developed a nonrelativistic, pure Coulomb field, mainly analytic, K -electron approximation; Johnson and Feiock [25] and especially Kissel [26] extended to realistic self-consistent Hartree-Fock potentials and performed a number of intensive numerical computations. The calculations are extremely difficult, usually considering the K -, and L -shell electrons and occasionally the M -shell electrons; a review is given by Kissel and Pratt [27].

Considering only free-particle intermediate states $|I\rangle$ and free-electron propagators, and assuming photon energies small compared to the electron rest energy $\omega \ll mc^2$, the initial and final electron energies differ little from mc^2 : $|E_i - mc^2| \ll mc^2$. The same assumption is applied to the energies of the intermediate states (i.e., $|E_I - mc^2| \ll mc^2$), and the above expression could be simplified to (Akhiezer and Berestetskii [21], p. 489).

$$A = \frac{ir_0}{2\pi\omega} e_i e_f^* \langle i | e^{iq \cdot r} | i \rangle \quad (2)$$

where $\mathbf{q} = \mathbf{k}_i - \mathbf{k}_f$ is the momentum transferred to the electron-atom system by the photon. Using Slater determinants for the initial states $|i\rangle$ the matrix element is given by a summation over form factors:

$$\langle i | e^{iq \cdot r} | i \rangle = f(q, Z), \quad (3)$$

$$f(q, Z) = 4\pi \sum_{i=1}^Z \int \rho_i(r) \frac{\sin(qr)}{qr} r^2 dr,$$

where $\rho_i(r)$ is the charge density of the i th electron and q is the momentum transfer.

This is the celebrated Franz [28] form-factor approximation to the Rayleigh scattering amplitudes. Brown, Peierles, and Woodward [22] tested this approximation and found it unsatisfactory. The problem with the form-factor approximation lies in the underlying assumption of a free-electron propagator in the intermediate states; that is, the atomic binding effects are neglected. Franz [29] himself introduced the *modified* form factor, which contains a binding correction, and its origin can be traced in the true electron propagator. The function $f(q, Z)$ above is replaced by the modification $g(q, Z)$:

$$g(q, Z) = 4\pi \sum_{i=1}^Z \int \rho_i(r) \frac{\sin(qr)}{qr} \frac{mc^2}{mc^2 - E_B^i - V(r)} r^2 dr,$$

$$q = (\omega/c) \sin(\theta/2),$$

$$A_{\perp} = -g(q, Z), \quad (4)$$

$$A_{\parallel} = -g(q, Z) \cos \theta,$$

$$\left[\frac{d\sigma}{d\Omega} \right]_{\text{Rayleigh}} = \frac{1}{2} r_0^2 (|A_{\parallel}|^2 + |A_{\perp}|^2),$$

where E_B^i is the binding energy of the i th electron, $\rho_i(r)$ is

its density, θ is the scattering angle, ω is the photon energy and r_0 is the classical electron radius.

Brown, Peierles, and Woodward [22] tested this approximation also and advocated its use over the regular form factors. As pointed out above the form-factor approximations are essentially nonrelativistic approximations. It was found that the modified form factor gives the best results when calculated with relativistic wave functions, and hence this approximation will be employed in the present work and is denoted as MRFF (modified relativistic form factor). This is another subtle correction to the nonrelativistic nature of the form-factor approximation.

III. RESULTS AND DISCUSSION

The experimental details of the present work are entirely similar to those presented in our previous publication [4]. Representative spectra of elastic scattered photons from the Pb target, at $\theta=1.02^\circ$ from the Ni(n,γ) source and at $\theta=1.80^\circ$ from the Fe(n,γ) source are presented in Fig. 1. The γ lines analyzed in the present experiment are marked by their energies in keV. Our experimental method is based on measuring Pb-to-C experimental ratios and using a theoretical C cross section to obtain Pb experimental cross sections. Representative C spectra at $\theta=1.80^\circ$ are presented in Ref. [4] and at $\theta=1.02^\circ$ in Ref. [30].

Data analysis details were published previously [4]. Table II summarizes the experimental results (all the cross sections in b/sr). Column 2 contains the experimental Pb-to-C ratios and their uncertainties. Column 3 is obtained multiplying the Pb-to-C ratio by the theoretical scattering cross section of C from Table I in Ref. [4].

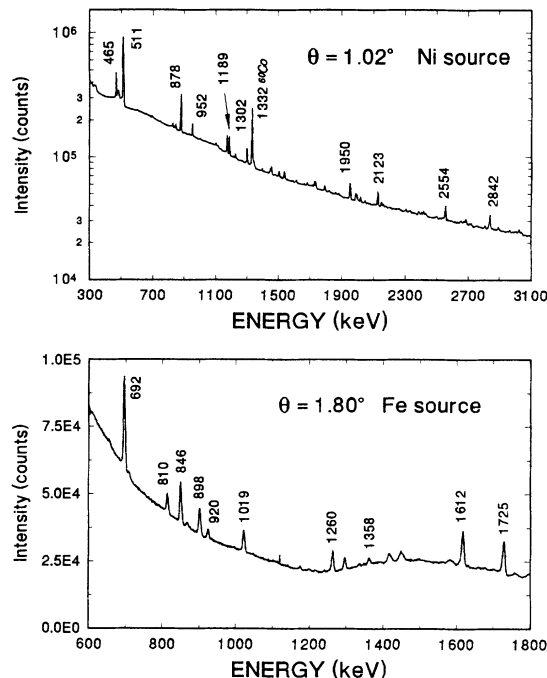


FIG. 1. Spectra of scattered photons from the Pb target [Ni(n,γ) and Fe(n,γ) sources] after background subtraction.

This is the elastic-scattering cross section measured in the present work. It contains both a coherent (Rayleigh) contribution and an incoherent one (Compton), un-separated from the former because of the small scattering angle (the maximum Compton shift at $\omega=2842$ keV, and $\theta=1.02^\circ$ is 2.5 keV, which is the comparable with the linewidth given by the detector resolution). Theoretical

TABLE II. Extraction of the Rayleigh cross section for Pb from the experimental Pb-to-C ratios (details in the text). The upper energy group refers to $\theta=1.02^\circ$, the lower one to $\theta=1.80^\circ$.

Energy (keV)	Experimental Pb-to-C ratio	Experimental Pb	Compton Pb	Experimental Rayleigh Pb	MRFF	Kane <i>et al.</i>
465	358.7 \pm 8.0%	251.7	1.34	250	269.2	269.9
878	240.7 \pm 4.0%	133.4	2.34	131	138.6	138.0
952	185.2 \pm 7.6%	101.5	2.49	99	124.4	124.0
1189	164.8 \pm 7.0%	87.8	2.89	85	90.2	88.0
1302	133.5 \pm 8.0%	70.2	3.06	67	76.8	75.7
1950	71.8 \pm 6.0%	35.6	3.80	32	34.0	33.1
2133	61.4 \pm 10.0%	30.1	3.96	26	28.3	27.5
2554	49.2 \pm 8.0%	23.7	4.34	19	19.5	18.1
2842	39.7 \pm 5.0%	19.1	4.55	14.5	16.1	14.3
692	186.0 \pm 3.9%	98.6	2.94	95	86.0	84.3
811	151.6 \pm 12.6%	78.5	3.22	75	64.9	63.2
847	130.7 \pm 5.4%	67.2	3.31	64	59.6	57.7
898	121.0 \pm 7.1%	61.7	3.41	58	53.0	51.2
920	99.6 \pm 15.1%	50.6	3.45	47	50.4	48.9
1019	87.7 \pm 6.3%	43.8	3.64	40	40.6	39.4
1261	59.7 \pm 5.1%	29.1	4.06	25	25.6	24.6
1359	52.7 \pm 15.7%	25.6	4.21	21	22.0	20.9
1613	27.1 \pm 1.6%	13.0	4.55	8.4	16.1	14.2
1725	47.6 \pm 2.7%	22.7	4.69	18	14.4	11.9

Compton cross sections for Pb are presented in column 4. They were obtained by multiplying the Klein-Nishina cross section with the incoherent scattering function values taken from the tables of Hubbell *et al.* [31]. The Compton contribution to the scattering cross sections is negligible at small momentum transfers and rises to 25% at larger ones. It can be safely subtracted in order to obtain the Rayleigh contribution. The experimental Rayleigh cross section for Pb is obtained by subtracting column 4 from column 3. In most cases the relative uncertainties of these cross sections are nearly the same as those of the Pb-to-C ratios of column 2. Finally the last two columns contain theoretical results: one based on the MRFF calculations of Schaupp *et al.* [32] and the other on the calculations found in Table 2.8 of Kane *et al.* [33].

Figure 2 presents a comparison between our results and the MRFF calculations. From the ratio between the two it can be seen that the agreement is good, with a majority of the experimental points lying within 6.5% of the theoretical line. Qualitatively we confirm also the fact found already in our *U* investigation [4], namely, the MRFF approximation exceeds the experimental points by 5-6%. The majority of the experimental points are below the MRFF line, except in the group around 1 \AA^{-1} . This discrepancy is hard to prove on each individual point, because experimental uncertainties are about 10%, but, as a general trend over all the data, it is quite clear. Like our *U* experiment the point at 1612 keV is singular in its big discrepancy with the theory and with neighboring experimental data (2842 keV at almost the same $q = 2.04 \text{ \AA}^{-1}$). We suspect that, at this energy, an anomalously large scattering from C is responsible for cross

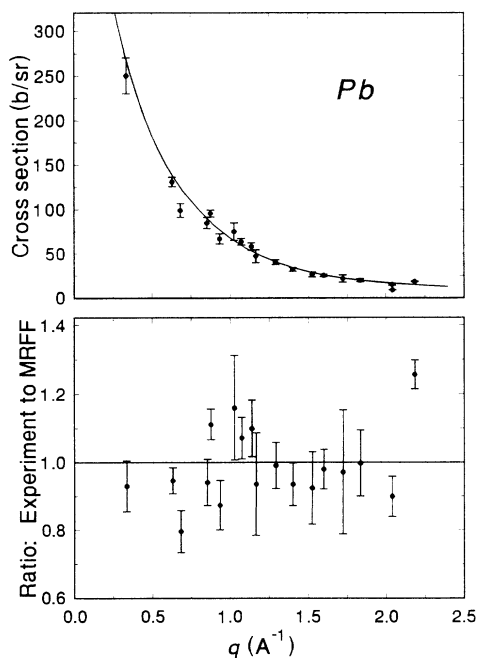


FIG. 2. Present results compared with MRFF calculations. Differential cross sections in the upper part and ratios between the two, in the lower part.

sections a factor of 2 smaller than the theoretical calculations. We do not have a reasonable explanation for this deviation.

Figure 3 presents a comparison between the data of Lestone *et al.* and the MRFF calculations. Above 1.2 \AA^{-1} the data of Lestone *et al.* show an impressive agreement with the theory. Below 1.2 \AA^{-1} there are sizable discrepancies which become greater on decreasing the momentum transfer, reaching 30% at 0.5 \AA^{-1} . Our experiment does not confirm the discrepancies found in the work of Lestone *et al.*, but only more mild and uniform deviations of about 5% as shown before.

The calculations of Kane *et al.* [33] are the most sophisticated Rayleigh calculations available. They include *K*- and *L*-electron *S*-matrix calculations, modified relativistic form factors for the other shells, imaginary-part amplitudes based on the photoelectric effect, and vanishing small contributions from Delbrück scattering, Thomson scattering, and nuclear resonance. Their Table 2.8 contains 385 points of calculated Pb cross sections at seven energies, in the range 59.5-1330 keV, and 55 angles. In comparing our result with the calculations of Kane *et al.* we encountered some difficulties. We extracted 89 points, in our range of momentum transfers, from their table. As can be seen from Fig. 4(a) these data present some clear irregularities. They are more obvious when the ratios between the calculations of Kane *et al.* and the MRFF calculations are plotted as in Fig. 4(b). All 16 points departing from the MRFF can be traced to calculations at 59.5 keV from 8° to 55° (i.e., momentum-transfer range $0.335\text{--}2.216 \text{ \AA}^{-1}$). For the other six energies and the same range of momentum transfer the agreement with the MRFF is very good. It seems therefore that the MRFF approximation breaks down at this energy. For our pur-

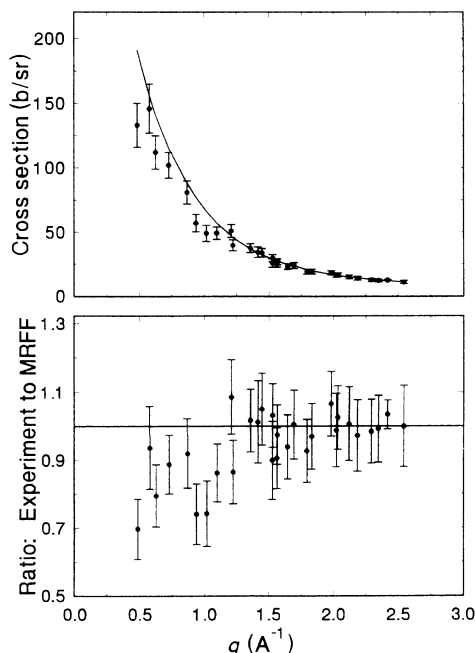


FIG. 3. Comparison between Lestone *et al.* [20] data and MRFF calculations (same as Fig. 2).

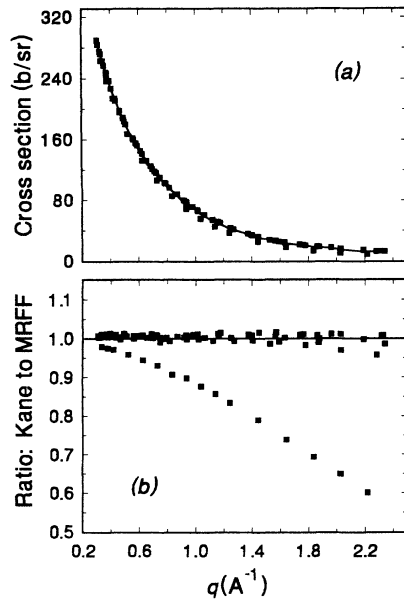


FIG. 4. Kane *et al.* [33] calculations: (a) all the calculated cross sections in the momentum transfer range $0.3\text{--}2.2 \text{ \AA}^{-1}$; (b) ratios to the MRFF calculations. The solid line in (a) is a cubic spline smoothed interpolating curve to Kane *et al.* calculations.

poses we constructed a cubic spline smoothed interpolating curve between all the points of Kane *et al.*, the solid line in Fig. 4(a). Using this interpolating curve the last column of Table II was extracted. As expected it agrees very well with the MRFF because most of the points of Kane *et al.* agree with the MRFF (within some range of fluctuation). Because of our good agreement with the MRFF, our data cannot confirm any breakdown in the MRFF approximation. But this is obvious because a breakdown in MRFF means separate dependence on ω and θ . As such, an experiment performed at $\omega=59.5$ keV is needed. Such an experiment is that of Eichler and de Barros [5]. Figure 5 shows comparisons between Eichler and de Barros data (in our range of momentum transfers) and (i) MRFF calculations—solid line; (ii) cu-

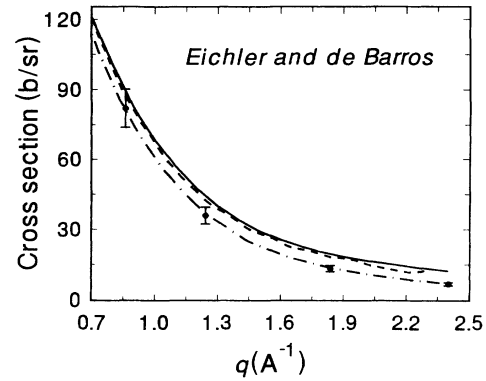


FIG. 5. Eichler and de Barros [5] data compared with (a) MRFF calculations, solid line; (b) smoothed interpolating curve to all Kane *et al.* calculations, dashed line; (c) Kane *et al.* calculations at 59.5 keV, dot-dashed line.

bic spline interpolating curve to all data of Kane *et al.*—dashed line; (iii) specific calculations of Kane *et al.* at 59.5 keV—dot dashed line. Obviously the Eichler and de Barros data confirm the breakdown in the MRFF approximation. This good agreement can be of course coincidental, and more experiments are needed in this region of energies to validate the breakdown of the MRFF.

IV. CONCLUSIONS

Rayleigh scattering cross sections from Pb were measured at 19 energies in the range $465\text{--}2842$ keV and momentum transfer range $0.3\text{--}2.2 \text{ \AA}^{-1}$. Good agreement with MRFF approximation is obtained, but, as a general trend, this approximation predicts a cross section that is too large by 5%. This is in agreement with our previous findings in Rayleigh scattering from U. A discrepancy with the MRFF, as large as 30% under 1.2 \AA^{-1} , previously reported by Lestone *et al.* [20], is not confirmed, but these two experiments are seen to be in overall qualitative agreement. Apparently the MRFF approximation breaks down under ≈ 100 keV.

[1] Lord Rayleigh, *Philos. Mag.* **41**, 107 (1871); **41**, 274 (1871); **47**, 275 (1899).
 [2] J. D. Jackson, *Classical Electrodynamics* (Wiley, New York, 1975), p. 423.
 [3] S. Kahane and R. Moreh, *Phys. Rev. C* **9**, 2384 (1974); S. Kahane, R. Moreh, and O. Shahal, *ibid.* **28**, 1519 (1983).
 [4] S. Kahane, O. Shahal, and R. Moreh, *Phys. Rev. A* **40**, 6950 (1989).
 [5] J. Eichler and S. de Barros, *Phys. Rev. A* **32**, 789 (1985).
 [6] M. Schumacher and A. Stoffregen, *Z. Phys. A* **283**, 15 (1977).
 [7] J. Eichler, S. de Barros, O. Gonçalves, and M. Gaspar, *Phys. Rev. A* **28**, 3656 (1983).
 [8] S. de Barros, J. Eichler, O. Gonçalves, and M. Gaspar, *Z. Naturforsch.* **36A**, 595 (1981).
 [9] M. S. Prasad, G. K. Raju, K. N. Murty, and V. Lakshminarayana, *J. Phys. B* **11**, 3969 (1978).

[10] M. Schumacher, *Phys. Rev.* **182**, 7 (1969).
 [11] D. Bradley and A. M. Ghose, *Phys. Rev. A* **33**, 191 (1986).
 [12] F. Smend, M. Schumacher, and I. Borchert, *Nucl. Phys. A* **213**, 309 (1973).
 [13] S. de Barros, J. Eichler, M. Gaspar, and O. Gonçalves, *Phys. Rev. C* **24**, 1795 (1981).
 [14] M. Schumacher, F. Smend, and I. Borchert, *Nucl. Phys. A* **206**, 531 (1973).
 [15] W. R. Dixon and R. S. Storey, *Can. J. Phys.* **46**, 1153 (1968).
 [16] G. Hardie, W. J. Mellow, and D. R. Schwandt, *Phys. Rev. C* **1**, 714 (1970).
 [17] G. Hardie, J. S. De Vries, and C. Chiang, *Phys. Rev. C* **3**, 1287 (1971).
 [18] G. Basavaraju, P. P. Kane, and K. M. Varier, *Pramana* **12**, 665 (1979).
 [19] P. P. Kane, J. Mahajani, G. Basavaraju, and A. K. Priya-

- darsini, Phys. Rev. A **28**, 1509 (1983).
- [20] J. P. Lestone, R. B. Taylor, P. Teansomprasomg, and I. B. Whittingham, Phys. Rev. A **37**, 3218 (1988).
- [21] A. I. Akhiezer and V. B. Berestetskii, Quantum Electrodynamics (Interscience, New York, 1965), p. 487.
- [22] G. E. Brown, R. E. Peierles, and J. B. Woodward, Proc. R. Soc. London Ser. A **227**, 51 (1955); G. E. Brown and D. F. Mayers, *ibid.* **234**, 384 (1956); **242**, 89 (1957).
- [23] H. Cornille and M. Chapdelaine, Nuovo Cimento **14**, 1386 (1959).
- [24] V. Florescu and M. Gavrila, Phys. Rev. A **14**, 211 (1976).
- [25] W. R. Johnson and F. D. Feiock, Phys. Rev. **168**, 22 (1968).
- [26] L. Kissel, Ph. D. thesis, University of Pittsburgh, 1977 (unpublished).
- [27] L. Kissel and R. H. Pratt, in *Atomic Inner-Shell Physics*, edited by B. Crasemann (Plenum, New York, 1985).
- [28] W. Franz, Z. Phys. **95**, 652 (1935).
- [29] W. Franz, Z. Phys. **98**, 314 (1936).
- [30] S. Kahane, R. Moreh, and O. Shahal, in *Neutron Capture Gamma-Ray Spectroscopy*, edited by R. E. Chrien and W. R. Kane (Plenum, New York, 1979), p. 643.
- [31] J. H. Hubbell, Wm. J. Veigele, E. A. Briggs, R. T. Brown, and D. T. Cromer, J. Phys. Chem. Ref. Data **4**, 471 (1975).
- [32] D. Schaupp, M. Schumacher, F. Smend, P. Rullhusen, and J. H. Hubbell, J. Phys. Chem. Ref. Data **12**, 467 (1983).
- [33] P. P. Kane, Lynn Kissel, R. H. Pratt, and S. C. Roy, Phys. Rep. **140**, 75 (1986).